ChemPlusChem

A Multidisciplinary Journal Centering on Chemistry

Chemistry Europe

European Chemical Societies Publishing

# Reprint

WILEY-VCH

# Binuclear Lanthanide(III) Complexes with Chiral Ligands: Dynamic Equilibria in Solution and Binding with Nucleotides Studied by Spectroscopic Methods

Jashobanta Sahoo,[a] Tao Wu,*[a] Blanka Klepetářová,[a] Jan Valenta,[b] and Petr Bouř[a]

Binuclear lanthanide complexes of Eu(III) and Sm(III) were obtained in the presence of chiral ligand 1,2-(*R*,*R*+*S*,*S*)-N,N′-bis (2-pyridylmethylene),2-diamine. An unusual structure of the Eu (III) compound with two lanthanide atoms connected through two chlorines was determined by X-ray crystallography. In solution, the dimer coexists with a monomeric complex, and the stability of the binuclear form depends on the solvent and concentration. The dimer-monomer equilibrium was monitored by circularly polarized luminescence (CPL) measured on a Raman optical activity (ROA) spectrometer, where both forms provided large CPL anisotropic ratios of up to $5.6\times10^{-2}$. Monomer formation was favored in water, whereas the dimer was stabilized in methanol. When mixed with adenosine phosphates, AMP gave much smaller CPL than ADP and ATP, indicating a high affinity of the Eu (III) complex for the phosphate group, which in connection with the ROA/CPL technique can be developed into a bioanalytical probe.

## Introduction

Lanthanide(III) probes generated considerable interest in bioanalyses and imaging due to their unique electronic structure, binding properties, and sensitivity to the environment.[1] Their luminescence is particularly sensitive to the neighborhood of the lanthanide core. In chiral species or in a chiral environment, circularly polarized luminescence (CPL, different emission of left- and right-circularly polarized light) reveals additional information about the stereochemistry in the excited states. Lanthanide unique luminescent properties, such as the highly specific CPL spectra, make them prone to many applications. CPL spectroscopy of customized lanthanide complexes has been used to identify and monitor various biomolecules,[2] or for time-gated contrast imaging.[3]

Analogous properties of lanthanide (III) and calcium ions are also interesting from the point of medicinal chemistry. Lanthanide complexes based on Schiff base ligands were found to be useful in cancer diagnosis and therapy, and for their antibacterial activity.[4] Most Schiff base ligands are easy to prepare, and they can be incorporated in complexes together with the lanthanide ions using usual synthetic procedures. Nevertheless, because of the high coordination numbers depending on the environment and solvent, the synthesis and structure characterization of lanthanide complexes remains challenging.

In the present study, we investigate structure and spectroscopic properties of two chiral binuclear lanthanide complexes (Scheme 1). They contain Schiff base N,N′-bis(2-pyridylmethylene),2-diamine as a chiral ligand, and a weak Ln–Ln bond is stabilized by two bridge chlorine atoms. The binuclear structure of the europium complex was determined by X-ray diffraction; a monomer-dimer equilibrium in solution could be observed using chiroptical spectroscopy.

The CPL spectra were measured with a Raman optical activity (ROA) spectrometer, as this option offers the possibility to detect weak signals, especially in aqueous solution, often undetectable on conventional CPL spectrometers.[5] The advantage of ROA is a strong laser excitation and sensitive detection

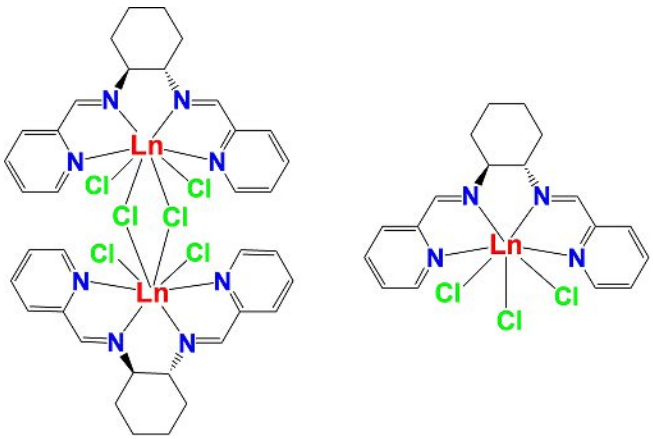


**Scheme 1.** Structure of the "dimer" binuclear complexes $[Ln(\mu\text{-}Cl)\mathbf{L}Cl_2]_2$; Ln=Eu, Sm; **L** = 1,2-(*R*,*R*+*S*,*S*)-N,N′-bis(2-pyridylmethylene),2-diamine (left) and the monomer (right).

[a] *Dr. J. Sahoo, Dr. T. Wu, Dr. B. Klepetářová, Prof. P. Bouř*
*Institute of Organic Chemistry and Biochemistry*
*Czech Academy of Sciences*
*Flemingovo náměstí 2, 16610 Prague (Czech Republic)*
*E-mail: wu@uochb.cas.cz*
[b] *Prof. J. Valenta*
*Faculty of Mathematics and Physics*
*Charles University*
*Ke Karlovu 3, 12116 Prague (Czech Republic)*

Supporting information for this article is available on the WWW under https://doi.org/10.1002/cplu.202000182
This article is part of a Special Collection on "Chemistry in the Czech Republic".

of the circular polarization. Particularly intense are the $^5D_0 \rightarrow {}^7F_0$ and $^5D_0 \rightarrow {}^7F_1$ europium transitions. Recently, we used the CPL/ROA technique for lanthanide-based sensing of biomolecules such as amino acids and proteins,[6] oligopeptides,[7] saccharides,[8] and nucleic acids.[9]

Compared to standard CPL data, the spectra are presented in the usual Raman format as dependent on the shift from the excitation laser line (532.0 nm in our case). The usual CPL dissymmetry factor $g_{lum} = 2(I_L - I_R)/(I_L + I_R)$ can be easily obtained from the ROA circular intensity difference, $CID = (I_R - I_L)/(I_R + I_L)$, as $g_{lum} = -2 \times CID$. $I_L$ and $I_R$ are intensities of the left- and right circularly polarized light.

## Results and Discussion

### Synthesis and ESI-MS

The ligand N,N′-bis(2-pyridylmethylene),2-diamine is soluble in organic solvents such as methanol and chloroform, but insoluble in water. The lanthanide complexes were found to be soluble both in methanol and water. MS spectra of [Eu(μ-Cl)**L**$Cl_2$]$_2$ in methanol solution contain **m/z** peaks attributable to two distinct cation species, molecular ion peak {[Eu(μ-Cl)**L**$Cl$]$_2Cl$}$^+$ (**m/z** = 1065.0 (found)/1065.2 (calc)) corresponding to dimeric complex, and [(Eu**L**$Cl_2$]$^+$ (**m/z** = 515.0 (found)/515.03(calcd)) as a fragmentation peak of monomeric complex. For aqueous solutions, only monomeric species was observed (Figure S5 in the supporting information), which is consistent with other data indicating that the binuclear dimer breaks down in aqueous solutions.

### X-ray Diffraction

Both ligand enantiomers crystallize in $P2_12_12_1$ chiral space group,[10] while [Eu(μ-Cl)(*R*,*R*-**L**)$Cl_2$)]$_2$ complex crystallizes in the $P2_1$ chiral space group (Table S1),[11] geometry of the complex is close to the $C_2$ symmetry. Each Eu(III) cation is eight-coordinated, bound to four nitrogen atoms of one tetradentate ligand and four chlorine anions (two of which form a bridge between the Eu(1) and Eu(2) ions, Figure 1). The Eu–N distances range from 2.487(5) to 2.612(5) Å. The longest Eu–Cl distances are between the Eu cations and the bridging chlorine anions (2.8208(16) Å and 2.8330(14) Å). The data are in agreement with the theoretical prediction; as usual, the calculated DFT bond lengths are slightly overestimated, see Table S2. The nitrogen atoms of the tetradentate ligands deviate slightly from the ideal square planar geometry (the maximum deviation from planarity being +0.106(5) Å for N(3) and −0.105(6) Å for N(2) in one ligand molecule and +0.145(5) Å for N(6) and −0.145(5) Å for N(7) in the other one). The distance of the Eu ions from the least-squares plane of the four coordinating nitrogen atoms is significantly longer (+0.7553(4) Å and −0.7533(4) Å for Eu(1) and Eu(2) ion respectively).

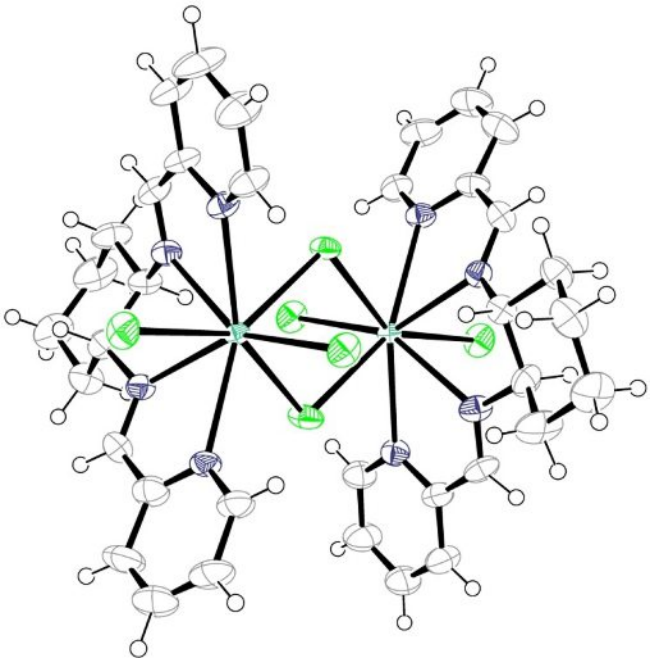

**Figure 1.** ORTEP[12] view of [Eu(μ-Cl)(*R*,*R*-**L**)$_2$)]$_2$, displacement ellipsoids shown with 50% probability.

### CPL Spectra

CPL spectra of the monomer and dimer Eu(III) complexes measured both in methanol and water solutions are plotted in Figures 2 and 3, respectively. The main CPL signals (Table 1), come from the $^5D_0 \rightarrow {}^7F_1$ (four bands in methanol 1778, 1893,

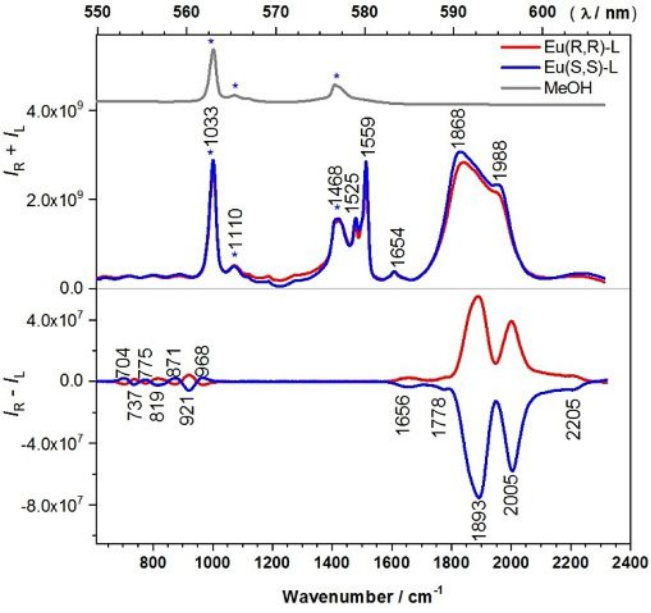


**Figure 2.** Raman/luminescence ($I_R + I_L$) and CPL ($I_R - I_L$) spectra of [Eu(μ-Cl)**L**$Cl_2$)]$_2$ enantiomers obtained for 4.7 mM solution in methanol, the accumulation time was 2 h, laser power was 80 mW with 532.0 nm excitation. The asterisks (*) indicates methanol bands, its Raman spectrum is plotted in grey.

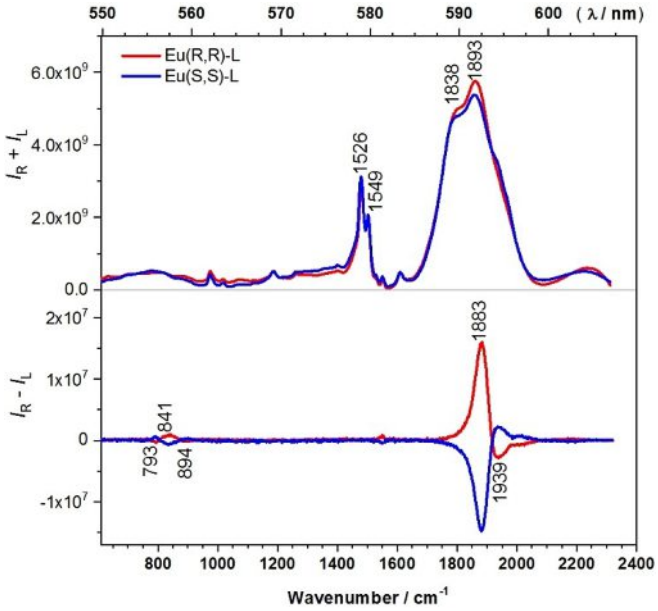


**Figure 3.** Total luminescence and CPL spectra of $[Eu(\mu\text{-}Cl)\mathbf{L}Cl_2)]_2$ enantiomers obtained in water (1.8 mM), with 2 h accumulation time, laser power was 800 mW with 532.0 nm excitation.

2005, and 2205 cm$^{-1}$; and two bands 1883 and 1939 cm$^{-1}$ in water) and $^5D_1 \rightarrow {}^7F_2$ (seven weak bands in methanol 704, 737, 775, 819, 871, 921 and 968 cm$^{-1}$; and three weak bands 793, 841 and 894 cm$^{-1}$ in water) transitions. Note that the transitions are further split into more bands due to the crystal field in the complex. The latter $^5D_1 \rightarrow {}^7F_2$ CPL bands are not accompanied by a visible luminescence signal, which can be explained by a high CPL/total luminescence ratio.[5c]

On the other hand, the $^5D_0 \rightarrow {}^7F_0$ transition is CPL silent, but measurable as two luminescence peaks (1525 and 1559 cm$^{-1}$ in methanol; 1526 and 1549 cm$^{-1}$ in water). The signal is very sensitive to decomposition of the binuclear complex into monomers. The band split visible in the ROA/CPL experiment is more difficult to measure on a normal fluorescence spectrometer due to the low resolution (centered at 615 nm, Figure S8). In methanol solution, the biggest band is located at 1559 cm$^{-1}$, while in water the 1526 cm$^{-1}$ band dominates. The maximum $g_{lum}$ value of $5.6\times10^{-2}$ of the $^5D_0 \rightarrow {}^7F_1$ transition in methanol decreases to about 10 times, to $5.9\times10^{-3}$ in water (Table 1).

A titration of $[Eu(\mu\text{-}Cl)(R,R\text{-}\mathbf{L})_2)]_2$ in methanol solution shows that at higher concentration (4.7 mM, stabilizing the dimer) luminescence and CPL intensities are much stronger than that at lower concentration (Figure 4, upper). Only positions of the two $^5D_0 \rightarrow {}^7F_0$ luminescence bands (1525 and 1559 cm$^{-1}$) almost do not change with concentration. CPL signals of $^5D_0 \rightarrow {}^7F_1$ decrease significantly, and the peak at 2001 cm$^{-1}$ almost disappears at concentration of 1.3 mM. The weakest CPL curve of $^5D_0 \rightarrow {}^7F_1$ transition is similar to that of previously reported mononuclear chiral Eu(III) complex derived from N,N′-bis(2-pyridylmethylene),2-diamine,[13] indicating that most of the binuclear complex dissociated into monomer under this condition.

**Table 1.** Assignment of observed Eu(III) and Sm(III) luminescence bands in methanol and water solutions.[a]

| $[Ln(\mu\text{-}Cl)\mathbf{L}Cl_2)]_2$ | δ [cm$^{-1}$] | λ [nm] | $\lvert g_{lum}\rvert$ | Transition[1b,5c] |
|---|---|---|---|---|
| Ln=Eu, | 2205 | 603 | | $^5D_0 \rightarrow {}^7F_1$ |
| in methanol | 2005, 1988 | 595 | $5.6\times10^{-2}$ | |
| | 1893, 1868 | 591 | $5.1\times10^{-2}$ | |
| | 1778 | 588 | | |
| | 1656, 1654 | 583 | | $^5D_1 \rightarrow {}^7F_3$ |
| | 1559 | 580 | | $^5D_0 \rightarrow {}^7F_0$ |
| | 1525 | 579 | | |
| | 968 | 561 | | $^5D_1 \rightarrow {}^7F_2$ |
| | 921 | 559 | | |
| | 871 | 558 | | |
| | 819 | 556 | | |
| | 775 | 555 | | |
| | 737 | 554 | | |
| | 704 | 553 | | |
| Ln=Eu, | 1939 | 593 | $5.9\times10^{-3}$ | $^5D_0 \rightarrow {}^7F_1$ |
| in water | 1893, 1883 | 591 | $1.4\times10^{-3}$ | |
| | 1838 | 590 | | |
| | 1559 | 580 | | $^5D_0 \rightarrow {}^7F_0$ |
| | 1525 | 579 | | |
| | 894 | 559 | | $^5D_1 \rightarrow {}^7F_2$ |
| | 841 | 557 | | |
| | 793 | 555 | | |
| Ln=Sm, | 2232 | 604 | | $^4G_{5/2} \rightarrow {}^6H_{7/2}$ |
| in methanol | 2131 | 600 | | $^4F_{3/2} \rightarrow {}^6H_{9/2}$ |
| | 2051 | 597 | | |
| | 1975 | 594 | | |
| | 1754 | 587 | | |
| | 1269 | 571 | | $^4G_{5/2} \rightarrow {}^6H_{5/2}$ |
| | 1021 | 562 | | $^4F_{3/2} \rightarrow {}^6H_{7/2}$ |
| | 930 | 560 | | |
| | 720 | 553 | | |
| Ln=Sm, | 2248 | 604 | | $^4G_{5/2} \rightarrow {}^6H_{7/2}$ |
| in water | 2035 | 597 | | $^4F_{3/2} \rightarrow {}^6H_{9/2}$ |
| | 1930 | 593 | | |
| | 1076 | 564 | | $^4G_{5/2} \rightarrow {}^6H_{5/2}$ |
| | 991 | 562 | | $^4F_{3/2} \rightarrow {}^6H_{7/2}$ |
| | 923 | 559 | | |

[a] $\lvert g_{lum}\rvert (= \lvert 2CID\rvert)$, Raman shift from the 532 nm laser frequency (δ/cm$^{-1}$) and corresponding wavelength (λ/nm).

In water, the relative intensity of the two luminescence bands of $^5D_0 \rightarrow {}^7F_0$ (1526 and 1549 cm$^{-1}$) also changes significantly. At 1549 cm$^{-1}$ luminescence becomes smaller compared to the peak at 1526 cm$^{-1}$ as concentration decreases. Only at higher concentration the CPL is similar (positive bands 1881 and 1976 cm$^{-1}$) to that in methanol (positive bands 1891 and 2001 cm$^{-1}$).

The concentration dependence indicates that in methanol the binuclear structure is prevalent, and decomposes to monomer at lower concentration. In water the binuclear structure is also stabilized at higher concentrations, but it dissociates into the monomer more quickly as the concentration decreases. This is consistent with the ESI-MS data, where in water the dimer peak was not observed at all (Figure S5).

Somewhat different data were obtained when europium was replaced by samarium. The X-ray data could not be obtained. Also the emission spectrum of the Sm (III) complex was invisible with the 532 nm excitation; it exhibits extremely short lifetime and low quantum efficiencies if measured on a FluoroMax-4 spectrometer (Horiba) (Figure S8, Table S3). CPL

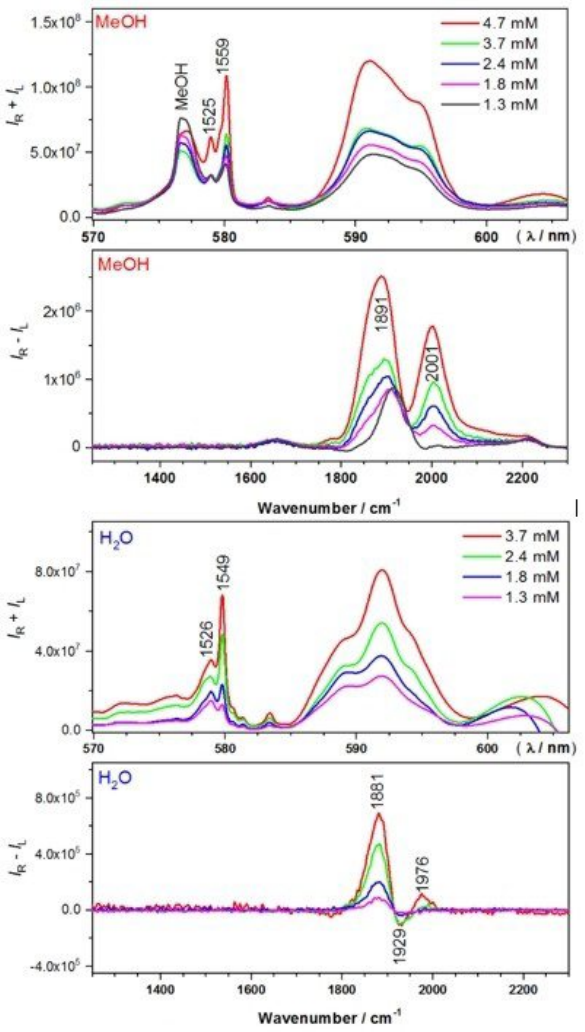


**Figure 4.** Normalized total luminescence and CPL spectra of [Eu(μ-Cl)(*R*,*R*-**L**)$_2$)]$_2$ for different concentrations in methanol (upper) and water (lower) solutions, with 10 min accumulation time.

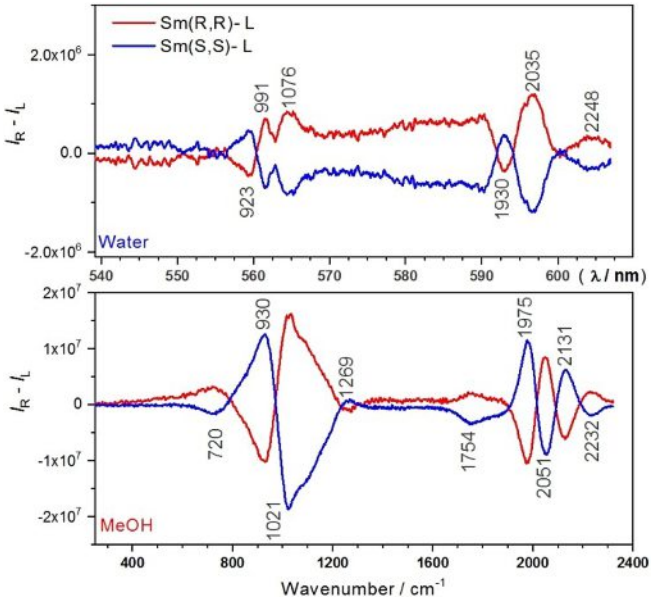


**Figure 5.** Normalized CPL spectra of [Sm(μ-Cl)**L**Cl$_2$)]$_2$ obtained in water (top) and methanol (bottom) solution (for concentration 4.2 mM in both cases, 24 and 16 h measurements for the water and methanol, respectively). Laser power was 120 mW in methanol and 600 mW in water with 532.0 nm excitation.

spectra in methanol and water solutions are presented in Figure 5. Similar as for Eu, collecting the weak CPL spectra of the Sm (III) complexes in water is not possible for conventional CPL instrument. As for Eu, the ESI-MS data indicate that the binuclear structure is prevalent in methanol (Figure S6), and monomeric structure dominates in water solutions (Figure S7). Also the CPL signal in methanol is stronger than for water, which was attributed to the equilibrium of the binuclear structure and monomer. The main CPL bands of Sm(III) transitions are listed in Table 1.

## CD Measurement and DFT calculations

Similar ECD spectra of [Eu(μ-Cl)(*R*,*R*-**L**)$_2$)]$_2$ and [Sm(μ-Cl)(*R*,*R*-**L**)$_2$)]$_2$ were observed in methanol solutions, stronger than for the free ligand (Figure S9, top), indicating that a similar dimer geometry is formed. The exciton coupling between the two monomeric units significantly enhances the dimer CD. The main spectra features are reasonably well simulated by the computation (Figure S9, bottom). The ECD intensity decreases significant in water solution (Figure S10) and becomes similar to that of free ligand, which confirms that under low concentration only the monomer is present.

Also IR and VCD spectra (Figure 6) of [Eu(μ-Cl)**L**Cl$_2$)]$_2$ enantiomers were measured in MeOH-d4 solutions at high concentrations (64 mM). Here, the binuclear geometry should

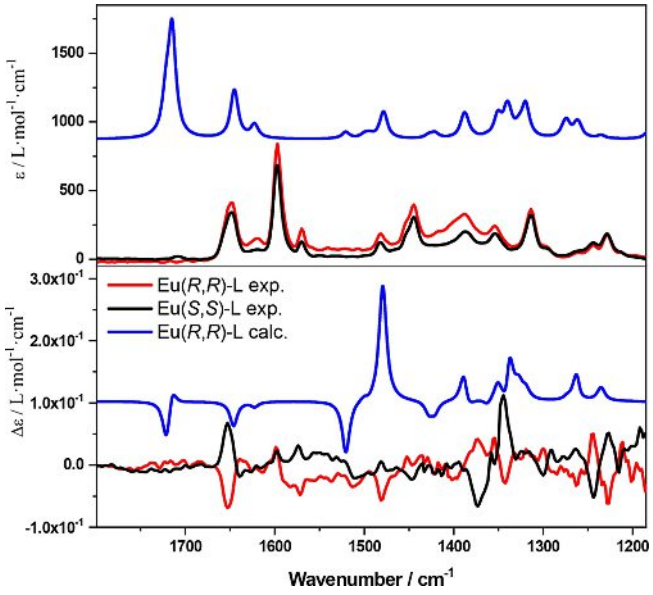


**Figure 6.** IR (upper) and VCD (lower) spectra of [Eu(μ-Cl$_2$)]$_2$ enantiomers (64 mM) measured in MeOH-d4 solution (red for *R*,*R* isomer; and green for *S*,*S* isomer) in comparison with DFT calculated *R*,*R* dimer (blue).

be prevalent, which is confirmed by comparison of the simulated IR spectrum to the experiment. Unfortunately, experimental VCD is weak and prone to artifacts, and a band-to-band comparison to the calculation is problematic.

The computation provides approximate formation energy of the complex, indicating that two monomers (Scheme 1) are slightly more convenient than the dimer, by 7.2 kcal/mol, which is in agreement with the dimer volatility observed in the titration experiments. This is consistent with computed electron density, which reveals very weak covalent character of the Eu–Eu, but also of the Eu–Cl bonds (Figure 7).

**NMR Spectra**. $^{1}$H NMR spectra of free ligand and the Eu(III) complex are plotted in Figure S11, Despite of paramagnetic coupling effect of the Eu(III) ion, proton shifts could be read. Due to the symmetry of the ligand, the aromatic protons (two pyridine rings) display multiple peaks centred around 8.51, 7.93, 7.82 and 7.39 ppm. The proton on the Schiff base C=N bond gives a single peak at 8.29 ppm. The chemical shifts of these protons change significantly in the presence of the Eu(III) ion. In $D_2O$, these peaks shifted to lower values and became broader single peaks (Figure S11B), because the coupling between protons in the pyridine ring was suppressed by Eu(III). The proton numbers obtained by NMR integration are similar to that of free ligand, indicating that the main form of the complex in $D_2O$ is a monomer. In deuterated methanol, the aromatic protons in the complex give multiple overlapped NMR bands (Figure S11C), indicating presence of the dimer. The $^{13}$C NMR spectrum of Eu(III) complex in $D_2O$ is also similar to the free ligand (Figure S12).

**Eu(III) Complex Binding with Adenosine Phosphates**. In aqueous solutions the unsaturated coordination number of Eu (III) in the monomeric complex Eu-**L**-$Cl_3$ (Scheme 1) offers many binding sites for other molecules. Three nucleotides, adenosine mono-, di-, and tri- phosphates (AMP, ADP, ATP) important in the cellular metabolism were selected for sensing studies. ROA-CPL spectra of the Eu(III) complex binding with adenosine phosphates in aqueous solutions are plotted in Figure 8. The luminescence bands of the Eu-nucleotide complexes (2200–1600 cm$^{-1}$) are almost identical except minor variances in intensity, probably caused by –OH groups of the phosphate and a quenching effect. The Raman signals of the nucleotide skeletons were too weak to be recognizable. The single luminescence band for $^{5}D_0 \rightarrow {}^{7}F_1$ in these Eu-nucleotides (1529 cm$^{-1}$ in AMP, 1521 cm$^{-1}$ in ADP and ATP) indicates that the structure of the Eu(III) complex is monomeric Eu-**L**-$Cl_3$ (Figure 3).

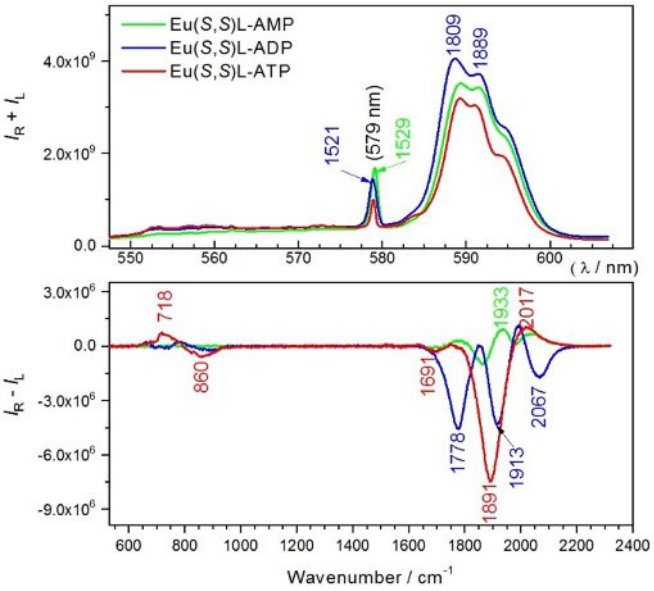


**Figure 8.** Total luminescence and CPL spectra of complex Eu-(*S,S*)-L (1 mM) chelating with AMP, ADP and ATP (4 mM) in water, with 1 h accumulation time. Laser power was 960 mW with 532.0 nm excitation.

Similarly as the Raman scattering, true vibrational ROA spectra of AMP, ADP, and ATP could not be measured under such low concentration.[14] In the region of 1170–620 cm$^{-1}$, CPL intensity of the Eu(III) $^{5}D_1 \rightarrow {}^{7}F_2$ transition was strongest in ATP, and weakest in AMP solution. The CPL intensity variation in the present of the three phosphates indicates that binding between Eu complex and nucleotides becomes stronger as the number of phosphate residues increases, i.e. the Eu binding with ATP is probably the strongest. The role of the adenosine group seems to be limited; the weakest CPL signal was observed in the [Eu-**L**]-AMP mixture.

The CPL spectral shape of [Eu-**L**]-ATP is similar to that for $Eu^{3+}$ aqua ions chelating with double stranded DNA.[9] Experiment with $EuCl_3$ and the three phosphates gave, however, a different CPL signal (Figure S13), revealing that the binding mode between [Eu-**L**]$^{3+}$ and $Eu^{3+}$ aqua ions are different. Titration of the nucleotides with Eu-**L**-$Cl_3$ were explored in Figures S14–S16. The Eu-**L**-$Cl_3$ solution began to precipitate when the Eu-**L**-$Cl_3$/AMP molar ratio was larger than 1:8. As the concentration of the nucleotides increased, no significant changes were observed in the luminescence and CPL spectra, except for intensity differences. No chirality unusual amplification was observed; maximum values of the $|g_{lum}|$ factor in these mixtures were either smaller or equivalent to those for the Eu (III) monomer complex.

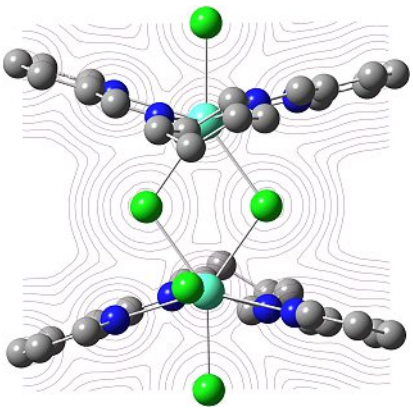

**Figure 7.** Contours of calculated electron density (ρ) in the dimer. At the midpoint between the Eu atoms, ρ ~ 0.013 atomic units. For comparison, the lowest density at the line between Eu and Cl atoms is ~0.025, typical value in C–C and C–H covalent bonds is ρ ~ 0.3.

## Conclusion

New Eu and Sm enantiomeric binuclear lanthanide complexes were prepared and characterized by various spectroscopic methods. The proximity of two lanthanide atoms bridged by chloride was for Eu confirmed by X-ray crystallography and computational modeling. An analogous structure is supposed for Sm. The CPL spectra were obtained with the aid of a ROA spectrometer, where even a weak CPL of Sm(III) could be observed. The binuclear (Eu…Eu or Sm…Sm) geometry was found to be slightly more stable in methanol solution than in water solutions, which was also confirmed by the NMR measurements. The binding of the monomeric Eu(III) complex to the adenosine phosphate could be followed as changes in the CPL band shapes. The affinity of the complex to the phosphate group can be perhaps explored in the future in biological studies. The results also manifest that the ROA technique is useful for lanthanide CPL measurement, even at weak emissions, and the polarized measurements can disclose more information than unpolarized (total) luminescence.

## Experimental Section

Detailed crystal structures, fluorescence decay lifetimes, ESI-MS spectra, fluorescence emission spectra, NMR spectra, experimental ECD spectra, and other CPL spectra are supplied in the Supporting Information.

All chemicals were purchased from Signal Aldrich. Elemental analyses were carried out by using a Perkin Elmer (PE) 2400 Series II CHNS/O Analyzer. Low resolution mass analyses were recorded by using the electron spray ionization mass spectroscopy (ESI-MS) technique with a Q-Tof micro (Waters) mass spectrometer and for high resolution mass spectroscopy (HRMS) using LTQ Orbitrap XL (Thermo Fisher Scientific) for all these complexes upon dissolving in methanol. $^{1}H$ and $^{13}C$ NMR spectra were measured with a Bruker Avance III™ HD 400 MHz spectrometer, at ambient temperature and using 5 mm diameter NMR tubes, with *S,S*-L ligand and dimer complex in deuterated methanol and monomer complex in deuterated water. The NMR measurements were carried out at least one hour after the sample was dissolved.

Chiral tetradentate ligands (*R,R*-L and *S,S*-L) were synthesized by condensing *R,R*- or *S,S*- diaminocyclohexane with 2-pyridine carboxaldehyde, following previously described procedure.[15] 0.292 g (0.001 mmol) of the ligand was dissolved in 40 ml of methanol, and solution of lanthanide(III) chloride hexahydrate (0.001 mmol) in 10 ml methanol was added gradually. The reaction mixture stirred for 8 h at room temperature, resulted light-yellow solution was evaporated under reduced pressure. Final solid powder was isolated using vacuum desiccator at room temperature for 48 h. ESI-MS (methanol, Scan ES+; *m/z*): $(L+H^{+})$ **m/z** = 293.2 (found)/293.18 (calc), $(L+Na^{+})$ **m/z** = 315.1 (found)/315.16 (calc) (Figure S3). The solid powder was further dissolved in methanol solution and suitable crystal for X-ray crystallography was obtained by slow evaporation of the solvent (Figures S1–2).

**[Eu(μ-Cl)$_2$L]$_2$**: yield 72 %, the powder product was recrystallized from methanol solution for spectroscopic measurement. Suitable crystal of complex [Eu(μ-Cl)(*R,R*-**L**)Cl$_2$)]$_2$ for X-ray crystallography produced by slow evaporation of the methanol solution. ESI-MS: {[Eu(μ-Cl)**L**Cl]$_2$Cl}$^{+}$, **m/z** = 1065.0 (found)/1065.2 (calc), [(Eu**L**Cl$_2$]$^{+}$ (**m/z** = 515.0 (found)/515.03(calcd)) (Figure S4). Elemental analysis: Calculated for $C_{36}H_{52}Cl_6Eu_2N_8O_6$. Calc.(Expt.); C, 35.75 (35.67), H, 4.33(4.19), N, 9.26 (9.62)%.

**[Sm(μ-Cl)$_2$L]$_2$**: yield 71 %, the powder product was recrystallized from methanol solution for spectroscopic measurement. ESI-MS: {[Sm(μ-Cl)**L**Cl]$_2$Cl}$^{+}$ **m/z** = 1063.0(found)/1063.03 (calc)); and [Sm**L**Cl$_2$]$^{+}$ (**m/z** = 514.0 (found)/514.03(calcd)). (Figure S6). Elemental analysis: Calculated for $C_{36}H_{50}Cl_6Sm_2N_8O_5$. Calc.(Expt.); C, 36.39 (36.31), H, 4.24(4.11), N, 9.43 (9.47)%.

**Electronic Circular Dichroism (ECD)**: The spectra were recorded with a Jasco J-815 spectrometer for methanol and water solutions in 0.1 mm quartz cell.

**Vibrational Circular Dichroism (VCD)**: The measurement was performed using a BioTools ChiralIR-2X instrument. The samples were placed in a $CaF_2$ cell with 0.1 mm spacer, the complex concentrations was 64 mM in deuterated methanol. Each spectrum was accumulated for 16 hours at 4 $cm^{-1}$ resolution. Absorption (IR) and VCD spectra of pure solvents were subtracted.

**Single Crystal X-ray Crystallography**: Single-crystal X-ray diffraction data for ligand *R,R*-and *S,S*-L and [Eu(μ-Cl)(*R,R*-**L**)Cl$_2$)]$_2$ were obtained on an Xcalibur X-ray diffractometer using monochromatized $Cu_{K\alpha}$ radiation ($\lambda = 1.54180$ Å) at 180 K. CrysAlisProCCD[16] was used for data collection, cell refinement and data reduction. The structures were solved by direct methods with SIR92[17] and refined by full-matrix least-squares on F with CRYSTALS.[18] All hydrogen atoms were found on difference Fourier map and recalculated into idealized position, the non-hydrogen atoms were refined with anisotropic displacement parameters. Summary of the crystal data for all three structures is given in Table S1. Disordered solvent molecules (methanol and/or water) were not included in the refinement and the disordered density was taken into account using the SQUEEZE procedure (from PLATON).[19] CCDC 1921619, 1921620 contains the supplementary crystallographic data for the chiral ligands *S,S*-L, *R,R*-L and 1921621 for [Eu(μ-Cl)(*R,R*-**L**)Cl$_2$)]$_2$.

**Emission Spectra**: Fluorescence measurements were realized on a FluoroMax-4 spectrometer (Horiba), the bandwidth for emission and excitation are adjusted for bandwidths of 5.0/5.0 nm with concentration $2\times10^{-5}$ M and path length about 1 cm.

**CPL Measurement**: Backscattering Raman and scattered circular polarization (SCP) ROA spectra (dominated by Eu TL and CPL) were acquired on a BioTools ROA spectrometer operating with laser excitation at 532 nm and resolution of 7 $cm^{-1}$. For the lanthanide CPL measurement the laser power at the sample was 20–600 mW, accumulation times varied dependent on the CPL intensity from 10 minutes to 24 hours. Concentrations were 1–4.7 mM for europium complex and 4.2 mM for samarium complex. The concentration of Eu(III) in adenosine phosphates solutions was 1 mM for Eu-**L**-$Cl_3$ and 2 mM for $EuCl_3$, and the laser power was 900–1000 mW. The intensities were normalized to the 1650 $cm^{-1}$ band, and a broad luminescence background coming from sample impurities was subtracted from the Raman signal. Usually, the experiments were repeated three times and no change in the spectra due to photolysis/decomposition was observed.

**Computations**: Initial [Eu(μ-Cl)(*R,R*-**L**)Cl$_2$)]$_2$ complex geometry was generated from crystal structure determined by X-ray crystallography, and optimized by the Gaussian 16 program[20] adopting the B3LYP functional and 6–31G(d,p) basis set (MWB28 pseudopotential basis set for Eu). The solvent was modelled by the conductor-like polarizable continuum solvent model (CPCM).[21]

## Acknowledgements

*The present study was supported by the Czech Science Foundation (1905974Y (T.W.), 1805770S (J.S.) and 20-10144 S (PB)), Ministry of Education (LTC17012 and CZ.02.1.01/0.0/0.0/16_019/0000729), and Charles University center UNCE/SCI/010 (J.V.). J.S. wishes to express his gratitude to Hindol college, Khajuriakata Higher Education Department, State Government of Odisha, India.*

## Conflict of Interest

*The authors declare no conflict of interest.*

**Keywords:** chiral ligands · circularly polarized luminescence · lanthanides · nucleotides · Raman optical activity

[1] a) M. C. Heffern, L. M. Matosziuk, T. J. Meade, *Chem. Rev.* **2014**, *114*, 4496–4539; b) J. C. G. Bunzli, *Chem. Rev.* **2010**, *110*, 2729–2755.
[2] a) G. Muller, *Dalton Trans.* **2009**, *38*, 9692–9707; b) R. Carr, N. H. Evans, D. Parker, *Chem. Soc. Rev.* **2012**, *41*, 7673–7686; c) F. Zinna, L. Di Bari, *Chirality* **2015**, *27*, 1–13; d) G. Longhi, E. Castiglioni, J. Koshoubu, G. Mazzeo, S. Abbate, *Chirality* **2016**, *28*, 696–707; e) K. Staszak, K. Wieszczycka, V. Marturano, B. Tylkowski, *Coord. Chem. Rev.* **2019**, *397*, 76–90.
[3] A. T. Frawley, R. Pal, D. Parker, *Chem. Commun.* **2016**, *52*, 13349–13352.
[4] M. T. Kaczmarek, M. Zabiszak, M. Nowak, R. Jastrzab, *Coord. Chem. Rev.* **2018**, *370*, 42–54.
[5] a) T. Wu, J. Kapitán, V. Mašek, P. Bouř, *Angew. Chem. Int. Ed.* **2015**, *54*, 14933–14936; *Angew. Chem.*, **2015**, *127*, 15146–15149; b) T. Wu, P. Bouř, *Chem. Commun.* **2018**, *54*, 1790–1792; c) T. Wu, J. Kapitán, V. Andrushchenko, P. Bouř, *Anal. Chem.* **2017**, *89*, 5043–5049.
[6] T. Wu, J. Kessler, P. Bouř, *Phys. Chem. Chem. Phys.* **2016**, *18*, 23803–23811.
[7] E. Brichtová, J. Hudecová, N. Vršková, J. Šebestík, P. Bouř, T. Wu, *Chem. Eur. J.* **2018**, *24*, 8664–8669.
[8] a) T. Wu, J. Kessler, J. Kaminský, P. Bouř, *Chem. Asian J.* **2018**, *13*, 3865–3870; b) T. Wu, J. Průša, J. Kessler, D. Dračínský, J. Valenta, P. Bouř, *Anal. Chem.* **2016**, *88*, 8878–8885.
[9] T. Wu, P. Bouř, V. Andrushchenko, *Sci. Rep.* **2019**, *9*, 1068.
[10] a) B. Liu, M.-J. Zhang, J. Cui, J. Zhu, *Acta Crystallogr.* **2006**, *E62*, o5359-o5360; b) Y. Zhang, L. Xiang, Q. Wang, X.-F. Duan, G. Zi, *Inorg. Chim. Acta* **2008**, *361*, 1246–1254.
[11] S. Kano, H. Nakano, M. Kojima, N. Baba, K. Nakajima, *Inorg. Chim. Acta* **2003**, *349*, 6–16.
[12] L. Farrugia, *J. Appl. Crystallogr.* **2012**, *45*, 849–854.
[13] M. Leonzio, M. Bettinelli, L. Arrico, M. Monari, L. Di Bari, F. Piccinelli, *Inorg. Chem.* **2018**, *57*, 10257–10264.
[14] S. Ostovarpour, E. W. Blanch, *Appl. Spectrosc.* **2012**, *66*, 289–293.
[15] a) F. Piccinelli, A. Melchior, A. Speghini, M. Monari, M. Tolazzi, M. Bettinelli, *Polyhedron* **2013**, *57*, 30–38; b) F. Piccinelli, A. Speghini, M. Monari, M. Bettinelli, *Inorg. Chim. Acta* **2012**, *385*, 65–72.
[16] CrysAlisPro, Oxford Diffraction, **2002**.
[17] A. Altomare, G. Cascarano, C. Giacovazzo, A. Guagliardi, M. C. Burla, G. Polidori, M. Camalli, *J. Appl. Crystallogr.* **1994**, *27*, 435.
[18] P. W. Betteridge, J. R. Carruthers, R. I. Cooper, K. Prout, D. J. Watkin, *J. Appl. Crystallogr.* **2003**, *36*, 1487.
[19] A. Spek, *Acta Crystallogr.* **2015**, *C71*, 9–18.
[20] M. J. Frisch, G. W. Trucks, H. B. Schlegel, G. E. Scuseria, M. A. Robb, J. R. Cheeseman, G. Scalmani, V. Barone, G. A. Petersson, H. Nakatsuji, X. Li, M. Caricato, A. V. Marenich, J. Bloino, B. G. Janesko, R. Gomperts, B. Mennucci, H. P. Hratchian, J. V. Ortiz, A. F. Izmaylov, J. L. Sonnenberg, Williams, F. Ding, F. Lipparini, F. Egidi, J. Goings, B. Peng, A. Petrone, T. Henderson, D. Ranasinghe, V. G. Zakrzewski, J. Gao, N. Rega, G. Zheng, W. Liang, M. Hada, M. Ehara, K. Toyota, R. Fukuda, J. Hasegawa, M. Ishida, T. Nakajima, Y. Honda, O. Kitao, H. Nakai, T. Vreven, K. Throssell, J. A. Montgomery Jr., J. E. Peralta, F. Ogliaro, M. J. Bearpark, J. J. Heyd, E. N. Brothers, K. N. Kudin, V. N. Staroverov, T. A. Keith, R. Kobayashi, J. Normand, K. Raghavachari, A. P. Rendell, J. C. Burant, S. S. Iyengar, J. Tomasi, M. Cossi, J. M. Millam, M. Klene, C. Adamo, R. Cammi, J. W. Ochterski, R. L. Martin, K. Morokuma, O. Farkas, J. B. Foresman, D. J. Fox, Wallingford, CT, **2016**.
[21] A. Klamt, *J. Phys. Chem.* **1995**, *99*, 2224–2235.

Manuscript received: March 6, 2020
Revised manuscript received: March 16, 2020
Accepted manuscript online: March 17, 2020